

# Chapter 1

## Tully-Fisher relation

Khaled Said

**Abstract** The observed radial velocity of a galaxy consists of two main components: the recession velocity caused by the smooth Hubble expansion and the peculiar velocity resulting from the gravitational attraction of growing structures due to matter density fluctuations. To isolate the recession velocity component and calculate the Hubble constant, accurate measurements of true distances are needed. The Tully-Fisher relation is an empirical correlation between the luminosity and rotational velocity of spiral galaxies that serves as a distance indicator to measure distances independent of redshift. The Tully-Fisher relation has played an important role in Hubble constant measurements since its inception. This chapter delves into the significance of the Tully-Fisher relation in such measurements and explores its implications. We begin by discussing the definition and historical background of the Tully-Fisher relation. We also explore the observational evidence supporting this relation and discuss its advantages and limitations. The chapter then focuses on the methodology of using the Tully-Fisher relation for Hubble constant measurements. This includes detailed explanations of calibration techniques and biases. We emphasize the advantages of utilizing the Tully-Fisher relation, such as its ability to provide accurate distance measurements even at significant redshift where other methods may encounter challenges.

---

Khaled Said (✉)

School of Mathematics and Physics, University of Queensland, Brisbane, QLD 4072, Australia,  
e-mail: [k.saidahmedsoliman@uq.edu.au](mailto:k.saidahmedsoliman@uq.edu.au)

## 1.1 Introduction

### 1.1.1 Description of the Tully-Fisher relation

The Tully-Fisher (TF) relation is an empirical relation that correlates the intrinsic brightness of a spiral galaxy, measured by its total luminosity, and its dynamical properties, measured by its rotational velocity. In 1977, Brent Tully and Richard Fisher proposed the use of this relation as a distance indicator based on their observations of spiral galaxies in the Virgo cluster [1]. The main idea behind distance indicators is to use distance-independent observables to predict a distance-dependent parameter, which can subsequently be compared with the corresponding observable to derive a distance estimate. In the case of the Tully-Fisher relation, the rotational velocity of a spiral galaxy serves as the distance-independent observable that is used to predict the total absolute luminosity, which is distance-dependent. The total luminosity can then be compared with apparent magnitude to measure distance via the distance modulus. The Tully-Fisher relation has since been extensively studied and refined [2, 3, 4, 5, 6, 7, 8, 9]. It has become a workhorse tool for measuring the distances and properties of galaxies, particularly in the context of large-scale structure surveys and cosmological studies [10, 11, 12, 13, 14, 15, 16].

### 1.1.2 Historical Background

The historical background of the Tully-Fisher relation can be traced back to the Great Debate in the 1920s, when Ernst Öpik used an expression between the observed rotational velocity and the absolute magnitude to measure the true distance to Andromeda [17]. This measurement helped to prove that Andromeda is an independent galaxy, not part of our own Milky Way Galaxy, as Shapley had thought.

More than 50 years later, Balkowski et al used the Nançay radio telescope in France to measure the line widths of a sample of 13 irregular and spiral galaxies [18]. They found a correlation between the line width and the luminosity but they did not apply this correlation as a distance indicator. This laid the foundation for the ground-breaking paper by Brent Tully and Richard Fisher in 1977 [1]. In their paper, Tully and Fisher used only inclined spiral galaxies and proposed the usage of the linear relation between H I profile and absolute magnitude as a distance indicator.

The publication of the Tully-Fisher relation in 1977 and the proposal to use it as a distance indicator was significant in many different ways. Firstly, it provided a robust new tool for measuring distance at redshifts that other methods such as Cepheid variable stars cannot reach. This opened up a whole range of large scale structure and cosmological studies. Notably, similar relations like the Fundamental Plane relation [19, 20] only emerged a decade later. Secondly, Tully and Fisher measured the Hubble constant  $H_0$  to be  $80 \text{ km s}^{-1} \text{ Mpc}^{-1}$  from the Virgo cluster and Ursa Major. This value was the first to deviate from the two mainstream values

at that time, low value of  $H_0 = 50 \text{ km s}^{-1}\text{Mpc}^{-1}$  which was promoted by Sandage and Tammann [21] and a higher value of  $H_0 = 100 \text{ km s}^{-1}\text{Mpc}^{-1}$  claimed by de Vaucouleurs [22]. This value is much closer to the value of Hubble constant that we know today.

### 1.1.3 Tully-Fisher relation in cosmology

The Tully-Fisher relation has been heavily used in measuring the Hubble constant  $H_0$ . Additionally, it has also been used as a valuable tool in many other cosmological studies<sup>1</sup>:

- **Cosmography:** The Tully-Fisher relation uses the maximum rotational velocity of a galaxy to predict its luminosity. This can be used to estimate the distance to the galaxy, and to measure its peculiar velocity. The peculiar velocity is the deviation from the smooth Hubble flow and can be used to reconstruct 3D maps of the density and velocity fields of the universe. In 2014, a team led by Brent Tully used the Wiener filter reconstruction [23] to recover the 3D density and velocity maps. They used these maps to set the borders of our home supercluster which they called Laniakea [24]. More recently, Alexandra Dupuy and H el ene Courtois used the full CosmicFlows-4 [25] catalog<sup>2</sup> to reconstruct the 3D density and velocity fields [26] and then redefine the boundaries of the Laniakea supercluster along with other structures such as Perseus-Pisces and Shapley [27].
- **Bulk Flow:** The bulk flow is the average peculiar velocity over a sphere of a given radius  $R$ . The theoretical expected value of this measurement relies on a model of a specific set of cosmological parameters, initial conditions and a chosen gravitational law [28]. In 2009, Watkins, Feldman and Hudson used the largest TF survey available at that time, the SFI++ survey [10], to measure the bulk flow of galaxies. They used a new method, the minimal variance estimator, and found a large bulk flow amplitude of  $431 \pm 102 \text{ km s}^{-1}$  within a scale of  $50 \text{ Mpc } h^{-1}$  [29]. The amplitude of this bulk flow is larger than expected from the  $\Lambda$ CDM model. More recently, several teams have used the state-of-the-art CosmicFlows-4 catalog [25], which contains more than 10,000 newly measured TF distances, to measure the bulk flow of galaxies. They have also found large bulk flows, arising on a much larger scale, that are higher than the expected value from the  $\Lambda$ CDM model [26, 30, 31]
- **Growth rate of structure:** Over the last three decades, many collaborations have started to test Einstein's general theory of relativity over a range of scales. One way to do that is by measuring the growth rate of cosmic structure, or  $f\sigma_8$ . This method is capable of measuring  $f\sigma_8$  at low redshifts ( $z < 0.1$ ), a range inacces-

<sup>1</sup> I do not intend to give a comprehensive review of all cosmological studies that used TF relation, but I will discuss a few examples before focusing on the role of TF relation in the  $H_0$  tension which is the main focus of this chapter.

<sup>2</sup> This catalog contains TF distances along with other distance indicators

sible to other methods such as the redshift space distortion. The growth rate can be constrained by comparing the density field from redshift surveys and peculiar velocity fields from TF surveys. The growth rate can then be parameterized as a function of the mass density parameter  $\Omega_m$  and the growth index  $\gamma$ , which is determined by the theory of gravity. In 2011, Marc Davis and others used the TF survey SFI++ to find a  $f\sigma_8$  value of  $0.31 \pm 0.06$  [32]. Other teams also used the TF SFI++ catalog and found a slightly higher value of  $0.401 \pm 0.024$  [33]. More recently, the CosmicFlows-4 catalog also was used to measure  $f\sigma_8$  and found a similar value of  $0.40 \pm 0.07$  [16].

- **Galaxy formation and evolution:** As an empirical relation between fundamental properties of galaxies, TF relation has been used to refine semi-analytical models and numerical simulations of galaxy formation and evolution [34, 35, 36].
- **Dark matter in galaxies:** The Tully-Fisher relation have also been used to probe the distribution and properties of dark matter in galaxies. Several studies put constraints on galaxy halo profiles by comparing the halo profile required by the Tully-Fisher relation to the density profile that is well-described by the Navarro-Frenk-White (NFW) profile [37, 38, 39].

## 1.2 The Tully-Fisher relation

### 1.2.1 How does it work?

The Tully-Fisher relation is defined and its usages in cosmology are discussed above. But how does it work in practice?

Building the Tully-Fisher relation requires two data sets: photometry and spectroscopy. Photometry provides a measurement of the galaxy's luminosity, which is the distance-dependent parameter in the TF relation. Spectroscopy provides a measurement of the galaxy's rotational velocity, which is the distance-independent parameter in the relation. The Tully-Fisher relation establishes the connection between the luminosity and rotational velocity of spiral galaxies. The TF relation is a secondary distance indicator and as the name suggests it requires calibration from a sample of galaxies with known distances usually coming from a primary distance indicator or a sample of cluster galaxies. Figure 1.1A represents the initial step in utilizing the TF relation for distance measurements. It shows a sample of galaxies with known rotational velocities and absolute magnitudes. The TF relation of the form:

$$M = a + b \log W \quad (1.1)$$

where  $M$  is the absolute magnitude,  $W$  represents the rotation,  $a$  and  $b$  are the TF slope and intercept, respectively, can be fit to that sample. This relation, which we often call a template relation (Fig. 1.1B), can be used to predict the absolute magnitude of a galaxy with unknown distance given a measurement of its rotational

velocity as shown in Fig. 1.1C. The predicted absolute magnitude can be compared to the galaxy’s apparent magnitude to yield the distance via the distance modulus as:

$$\mu = m - M(W). \quad (1.2)$$

where  $\mu$  is the distance modulus,  $m$  is the apparent magnitude, and  $M(W)$  is the predicted absolute magnitude of a galaxy from the TF relation given its rotational velocity

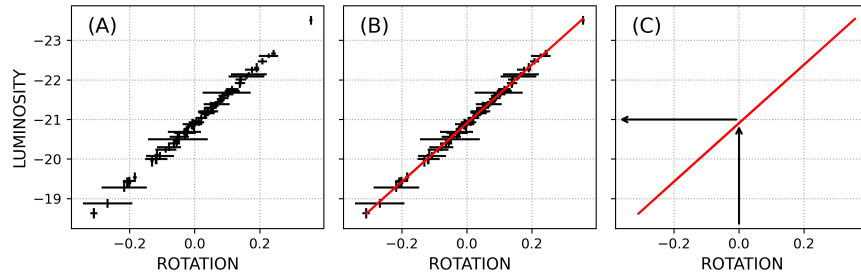


Fig. 1.1: Illustrating how the Tully-Fisher relation combines photometric and spectroscopic data to enable the estimation of galaxy distance. In order to use the Tully-Fisher relation to measure distances, we need to build something called template relation. (A) shows a sample of galaxies with known rotation velocity, apparent magnitude, and distances which allows the determination of luminosity. (B) By fitting the TF relation to this sample, a template relation is derived. This establishes the correlation between the absolute magnitude and the rotational velocity of galaxies. (C) Applying the Tully-Fisher template to a galaxy of unknown distance, the absolute magnitude can be estimated based on its measured rotational velocity.

It is important to note that the derived template relation is not a universal relation. Instead, the data, parameters, and corrections used in the measurements of the TF distances should be consistent with those used in building the TF template relation. This has encouraged many teams to derive their own template relations instead of using an existing one. In the past few decades, different measurements, wavelengths, and methodologies have been used to do this. For example, shortly after the inception of the TF relation, several studies began to use near-infrared (NIR) bands because they suffer less than optical bands from dust extinction (both internal and external) and are more sensitive to stellar mass [40, 11, 9]. Other groups used isophotal magnitudes instead of total magnitudes to extend the Tully-Fisher studies into the Zone of Avoidance around the plane of the Milky Way [41, 42].

In terms of spectroscopy, many parameters have been used in an attempt to minimise the intrinsic scatter of the TF relation. Many teams have used the 20% HI line

width (the width measured at 20% of the peak flux of the H I profile) including the original TF relation [1, 43, 44], while others suggested using the width measured at 50% instead [45, 46, 47, 48]. Furthermore, other teams suggest that the flat part of the optical rotation curve is the best proxy for the rotational velocity, and they have shown that it does indeed yield the tightest Tully-Fisher relation [49, 50].

Different methodologies have been used to extract the best-fitting parameters for the Tully-Fisher relation by applying different fitting procedures. In an attempt to overcome the Malmquist bias, Renée C. Kraan-Korteweg and others proposed the use of the inverse TF relation, which only takes into account the errors on the x-axis (rotational velocity) [4]. Since then, many teams have used both direct and inverse fitting procedures in their analyses [51, 52]. Other teams have used bivariate forms that take into account errors in both the x- and y-axes [45, 11, 9, 48]. Given the scatter in TF relation, a suggestion has been made to use a Bayesian mixture model, which is less biased by outliers [53].

In summary, the Tully-Fisher relation has been observed to hold over a wide range of applications, including different parameters, methodologies, and wavelengths. This suggests that the TF relation is one of the most robust and powerful tools for measuring galaxy distances.

### 1.2.2 Theoretical basis

The physical origin of the Tully-Fisher relation is still not fully understood, but it is certainly rooted in the physics of gravity and the dynamics of galactic rotation. The TF relation links the mass of a galaxy (characterized by the luminosity) to its dynamics (characterized by the rotational velocity). Specifically, it is based on the idea that the rotation velocity of a galaxy is related to the mass contained within a certain radius from the galaxy's center, known as the circular velocity.

Michael Strauss and Jeffrey Willick provided a widely accepted theoretical explanation<sup>3</sup> for the Tully-Fisher relation in their 1995 review [54]. They wrote that by equating the centrifugal force of an object moving in a circle of radius  $r$  to the gravitational attraction on the same object due to the mass inside a sphere of radius  $r$ , one can write

$$V_{\text{rot}}^2 \propto \frac{M}{r} \quad (1.3)$$

where  $V_{\text{rot}}$  is the rotational velocity,  $M$  is the mass within a sphere of radius  $r$ , and  $r$  is the distance from the galaxy's center. Then, assuming a constant value for both the mass-to-light ratio ( $M/L$ ) and mean surface brightness for spirals, one can obtain that

---

<sup>3</sup> This was not the first such explanation, but it was particularly clear.

$$L \propto V_{\text{rot}}^4 \quad (1.4)$$

However, most Tully-Fisher studies have derived a power-law exponent that deviates from this theoretical explanation. This is usually attributed to the complication of the dark matter halo that surrounds a galaxy [55]. Early near-infrared Tully-Fisher analyses showed that the complications of halo mass could be avoided, and indeed derived a power-law exponent that was closer to the theoretical expectation [40]. However, their conclusion has been contradicted by many larger subsequent surveys [45, 11].

In 2000, Stacy McGaugh and his team investigated the deviation of dwarf faint galaxies from the linear Tully-Fisher relation [6]. They found that the linear TF relation could be restored if they used the sum of both stellar and gas mass components instead of luminosity. This relation takes the form

$$M_d \propto V_{\text{rot}}^4 \quad (1.5)$$

where  $M_d$  is the sum of stellar and gas masses,

$$M_d = M_* + M_{\text{gas}}. \quad (1.6)$$

Not only did they establish the baryonic TF relation as the fundamental relation, but they also found that the intrinsic scatter was smaller than the original TF relation. This result can be simply explained if we suppose that this estimate of the baryonic mass is a better proxy for the true total mass than the luminosity or the stellar mass alone.

This result, at first glance, may seem to support the Modified Newtonian Dynamics (MOND: [56]) as an alternative to dark matter. MOND is a theory of gravity that modifies Newtonian dynamics. In MOND, the baryonic mass is actually the total mass, which means that the baryonic TF relation is the fundamental TF relation. However, it is important to note that Modified Newtonian Dynamics (MOND) has its own critics [57, 58]. We refer the reader to the literature for more information about the debate between MOND and Cold Dark Matter.

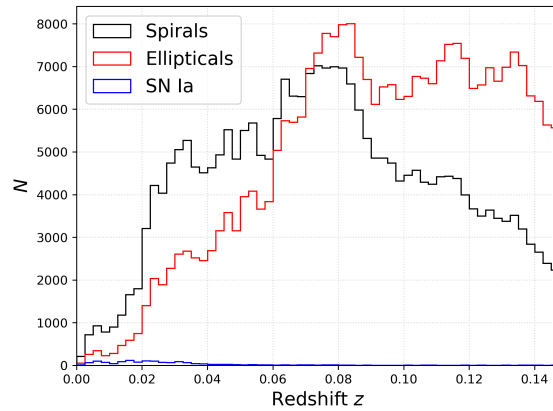
One important theoretical development in recent years has been the use of hydrodynamic simulations to study the formation and evolution of galaxies in a cosmological context [35, 59]. These simulations incorporate the effects of gravity, gas dynamics, star formation, and feedback, and have been shown to predict the Tully-Fisher relation in different environments and at different redshifts better than semi-analytical models [60].

### 1.2.3 Advantages and limitations

The Tully-Fisher relation has several advantages as a tool for measuring distances of galaxies. The first and main advantage is its simplicity and robustness. The TF relation provides a linear correlation between only two easily measurable galaxy properties, luminosity and rotational velocity. Several studies have shown that, unlike other distance indicators, the scatter of the TF relation is relatively insensitive to other galaxy properties [61, 8, 62]. This makes the TF relation a fundamental, robust and reliable tool for measuring distances.

Another advantage of the Tully-Fisher relation is that it uses spiral galaxies, which are the most numerous type of galaxies at low redshifts ( $z < 0.07$ ). This makes it a convenient tool for measuring peculiar velocities at these redshifts, where the true distances can be determined. Beyond this redshift, it is more difficult to obtain accurate peculiar velocities as the errors in measuring these velocities from distance indicators scale with redshift.

**Fig. 1.2** The redshift distribution of spiral (black) and elliptical (red) galaxies in the SDSS survey, as well as the redshift distribution of the state-of-the-art SN Ia from Pantheon+ (blue), up to redshift  $z < 0.15$ . The number of galaxies per 0.0025 redshift bin is shown.



In Figure 1.2, I show the redshift distribution of spiral and elliptical galaxies from the SDSS survey DR14 [63]. I separated spirals from ellipticals using the galaxy zoo catalog [64]. I also over plot the redshift distribution of the state-of-the-art Pantheon+ sample [65, 66]. I used only the redshift below  $z < 0.15$ , as this is the range used for Hubble constant ( $H_0$ ) measurements [67]. It is clear that spiral galaxies (Tully-Fisher galaxies) are the most numerous type at low redshift ( $z < 0.07$ ), with a mean redshift of  $z = 0.077$ . This makes TF relation one of the most precise tools for measuring  $H_0$  at this redshift.

However, there are also some limitations to the Tully-Fisher relation as a tool for distance measurements. One of the main limitations of the TF relation is its intrinsic scatter. This scatter can lead to errors of around  $\sim 20\%$  in distance measurements. The baryonic Tully-Fisher relation is often shown to be a tighter relation than the TF relation, with a much smaller intrinsic scatter [68, 69]. However, measuring the



sum of the stellar and gas components is much more difficult than measuring just the luminosity of a galaxy. This adds a lot of observational uncertainties to the baryonic TF relation.

Another limitation of the Tully-Fisher relation and a significant source of uncertainty is the inclination of galaxies. The inclination of a spiral galaxy affects both TF parameters. It affects the derived maximum rotational velocity during the process of correcting the observed line width for projection effects (i.e. to edge-on orientation). Additionally, to correct the magnitude for the internal extinction, one needs to use the inclination to account for the path-length of the light through the galaxy. Therefore, inclination errors lead to correlated errors in the two TF parameters that have the same sense (qualitatively) as errors in distance, so an error in inclination is (at least partly) degenerate with an error in distance. Most Tully-Fisher surveys select only edge-on galaxies by applying a cut to inclinations in an attempt to minimize the line width correction. Although this seems like the right thing to do, inaccurate inclinations will lead to a selection bias in the TF distance. This is because galaxies with inaccurate inclinations may be excluded or included in the survey, depending on whether their inclinations are overestimated or underestimated. Furthermore, edge-on galaxies are subject to higher internal extinction, which means that more light is blocked by dust and gas inside the galaxy. This results in a dimmer magnitude, and thus a larger correction is needed to correct for the extinction. Some studies have even suggested that when the inclination measurements have errors larger than 10 degrees, it may be more prudent to omit inclinations entirely rather than assuming them to be exact [70].

Selection effects and Malmquist bias are other limitations of the TF relation. However, these limitations are not specific to the TF relation, as they affect all distance indicators.

### 1.3 The Role of the Tully-Fisher relation in $H_0$ Measurements

The methodology for using the Tully-Fisher relation in  $H_0$  measurements typically involves the following steps. First, a sample of galaxies with well-measured rotational velocities and luminosities (for TFR) or masses (for the BTFR) is selected (see Fig. 1.1A). These galaxies are typically chosen to be representative of the population of galaxies being studied. Next, the Tully-Fisher relation is calibrated for this sample of galaxies. This involves measuring the slope, intercept, and scatter of the relation for the sample, and correcting for any systematic biases or selection effects (see Fig. 1.1B). Once the Tully-Fisher relation has been calibrated for the sample, it can be used to infer the distances to other galaxies with similar properties (see Fig. 1.1C). The final step is measuring  $H_0$ , which can be done by plotting the derived TF distances against redshifts.

This methodology has been used in a number of studies to estimate the value of the Hubble constant ( $H_0$ ). In 1977, Tully and Fisher applied their newly discovered Tully-Fisher relation to derive distances to the Virgo and Ursa Major clusters. They

measured a Hubble constant of  $H_0 = 84 \text{ km s}^{-1} \text{ Mpc}^{-1}$  for Virgo and  $H_0 = 75 \text{ km s}^{-1} \text{ Mpc}^{-1}$  for Ursa Major. They conclude a preliminary value for the Hubble constant of  $H_0 = 80 \text{ km s}^{-1} \text{ Mpc}^{-1}$ . Although they called it preliminary and did not propagate their distance error to the Hubble constant value, we know today that it was the most accurate result at that time.

In 1983, Visvanathan used the Tully-Fisher relation to measure distances to 52 cluster spiral galaxies. They found that the Hubble constant derived from nearby clusters varied from 58.5 to 83.5, but the range was much smaller for distant clusters, between 76.3 and 78.9  $\text{km s}^{-1} \text{ Mpc}^{-1}$ . Visvanathan concluded that the best fit value for the Hubble constant from all clusters in their study was  $H_0 = 74.4 \pm 11 \text{ km s}^{-1} \text{ Mpc}^{-1}$  [71]. That result is very close to the value of  $H_0$  we have today.

Shortly after, Sandage and Tammann used the Tully-Fisher relation in the infrared (IR) and blue bands to estimate distances to galaxies in the Virgo and Coma clusters, respectively. Their analysis gave a lower value of the Hubble constant  $H_0 = 55 \pm 9 \text{ km s}^{-1} \text{ Mpc}^{-1}$  [72]. This result aligned with their previous measurement of  $H_0 = 50 \pm 7 \text{ km s}^{-1} \text{ Mpc}^{-1}$  obtained through Type I supernovae [73].

Aaronson led a team in 1986 to derive distances to 10 galaxy clusters using the infrared Tully-Fisher relation. They stated that the current evidence favors a large value for  $H_0$  of  $90 \text{ km s}^{-1} \text{ Mpc}^{-1}$  [74]. In two subsequent studies, Bottinelli led a team to use the infrared Tully-Fisher relation to derive distances to galaxy clusters. They concluded that the  $H_0$  lies between 70 and  $75 \text{ km s}^{-1} \text{ Mpc}^{-1}$ . During the same time, Renée C. Kraan-Korteweg and others derived distances to a larger sample of 82 cluster galaxies using both the infrared Tully-Fisher relation and the optical Tully-Fisher relation. They found that their data is consistent with a Hubble constant of  $H_0 = 56.6 \pm 0.9 \text{ km s}^{-1} \text{ Mpc}^{-1}$  [75]. However, this low value was contradicted by three studies. One study used the TF relation to measure distances to Virgo and Ursa Major clusters, and derived a value of  $H_0 = 85 \pm 10 \text{ km s}^{-1} \text{ Mpc}^{-1}$  [43]. The other two studies derived distances to the Coma cluster, and also found a higher value of  $H_0 \approx 90 \text{ km s}^{-1} \text{ Mpc}^{-1}$  [76, 77]. Bureau, Mould, and Staveley-Smith [78] used the Tully-Fisher relation to measure distances to galaxies in the Fornax cluster, and derived a value of  $H_0 = 74 \pm 11 \text{ km s}^{-1} \text{ Mpc}^{-1}$ .

This significant discrepancy in these early measurements can be attributed to various factors, including the challenge of sample incompleteness correction and the absence of reliable distances to nearby objects for use as a calibration sample.

The Hubble Space Telescope Key Project on the Extragalactic Distance Scale used Cepheid distances to re-calibrate the Tully-Fisher relation. In a series of papers, they found results consistent with a value of  $H_0$  of  $71 \pm 4 \text{ km s}^{-1} \text{ Mpc}^{-1}$  [79, 80, 81].

The Cosmicflows project combines distances measured through various methods, including the Tully-Fisher relation, surveys, and collaborations. This project has made significant contributions to measuring the Hubble constant, consistently obtaining values in the range of  $74 \pm 4$  to  $76 \pm 1 \text{ km s}^{-1} \text{ Mpc}^{-1}$  over an extended period [82, 83, 84, 85, 86, 87, 88, 26]

Figure 1.3 shows a graphical representation of the published efforts to measure the Hubble constant ( $H_0$ ) using the Tully-Fisher relation. The red band shows the the most recent result of Hubble constant and its associated errors measured using

Type Ia supernovae by the SH0ES team in 2022 [89]. Additionally, the blue band represent the Hubble constant value and its associated error from the CMB measured by the Planck Collaboration in 2020 [90]. The figure shows a lot of scatter in the TF results prior to 2000 with some unrealistically optimistic uncertainties. However, after 2000, the results seem consistent and in more agreement with the value derived by the SH0ES team in 2022 [89] than the CMB value by the Planck Collaboration in 2020 [90]. Table 1.1 provides a summary of the results from these studies.

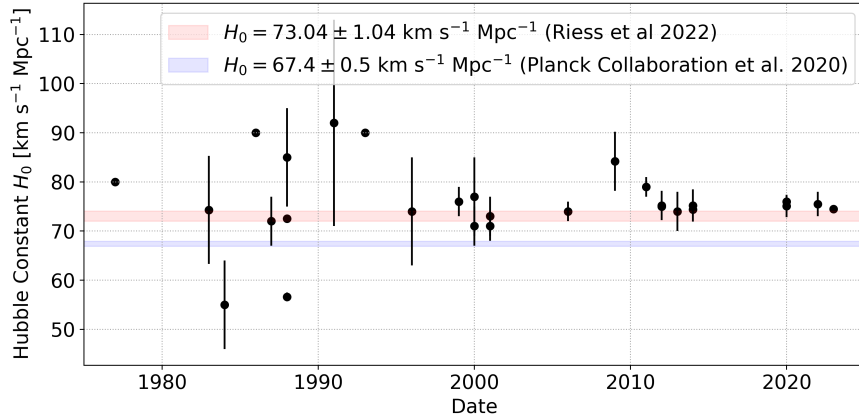


Fig. 1.3: A sample of published Hubble constant ( $H_0$ ) measurements using Tully-Fisher relation spanning from 1977 to 2023. Most of these measurements are obtained by different teams using different data given in table 1.1. The red band highlights the most recent Hubble constant value and its associated uncertainty from the baseline results of the Cepheid-SN Ia sample by the SH0ES team [89]. The blue band represents the Hubble constant value reported by Planck Collaboration 2020 [90]. The majority of the data points align closely with the red band, particularly from 2000 onward. It is important to note that this sample of data is just a subset from the literature and additional studies may already exist beyond those represented here.

In summary, the Tully-Fisher relation has been used for decades to estimate distances to galaxies and to measure the Hubble constant. Although Tully-Fisher measurements of  $H_0$  have shown a lot of scatter prior to 2000, they have been consistent since then with a value of  $H_0$  that agrees with the other low-redshift probes.

Table 1.1: Evolution of published Hubble constant values from the Tully-Fisher relation (1977-2023)

Date	$H_0$	Ref.		Date	$H_0$	Ref.
1977	80.0	[1]		2001	$71.0 \pm 3.0$	[81]
1983	$74.3 \pm 11.0$	[71]		2001	$73.0 \pm 4.0$	[91]
1984	$55.0 \pm 9.0$	[72]		2006	$74.0 \pm 2.0$	[46]
1986	90.0	[74]		2009	$84.2 \pm 6.0$	[92]
1987	$72.0 \pm 5.0$	[93]		2011	$79.0 \pm 2.0$	[94]
1988	$85.0 \pm 10.0$	[43]		2012	75.0	[82]
1988	72.5	[95]		2012	$75.2 \pm 3.0$	[83]
1988	$56.6 \pm 0.9$	[75]		2013	$74.0 \pm 4.0$	[84]
1991	$92.0 \pm 21.0$	[76]		2014	$74.4 \pm 1.0$	[85]
1993	90.0	[77]		2014	$75.2 \pm 3.3$	[86]
1996	$74.0 \pm 11.0$	[78]		2020	$75.1 \pm 2.3$	[96]
1999	$76.0 \pm 3.0$	[79]		2020	$76.0 \pm 1.1$	[87]
2000	$77.0 \pm 8.0$	[97]		2022	$75.5 \pm 2.5$	[88]
2000	$71.0 \pm 4.0$	[80]		2023	$74.5 \pm 0.1$	[26]

<sup>a</sup> This is just a subset of the published Hubble constant values using TF relation, and additional studies may already exist beyond those represented here.

## 1.4 Future Prospects

The largest homogeneous Tully-Fisher sample currently exists is the CosmicFlows-4 survey [87]. This survey includes 10,000 TF distances. Imminent surveys such as DESI [98] and WALLABY [15] will provide 50,000 and 200,000 TF distances, respectively, over the coming few years. With approximately 20% TF distance errors for about 250,000 galaxies covering a significant portion of the sky up to redshift  $z \approx 0.1$ , both random and systematic errors in  $H_0$  from large-scale structure will be considerably smaller compared to the most optimistic uncertainties associated with other low-redshift probes.

**Acknowledgements** KS acknowledges support from the Australian Government through the Australian Research Council’s Laureate Fellowship funding scheme (project FL180100168). I would like to express my gratitude to Tamara Davis and Matthew Colless for their valuable feedback on the initial draft of this review.

## References

1. R. B. Tully and J. R. Fisher. A new method of determining distances to galaxies. *A&A*, 54:661–673, February 1977.
2. J. Silk. Feedback, Disk Self-Regulation, and Galaxy Formation. *ApJ*, 481:703–709, May 1997.
3. V. Avila-Reese et al. On the Formation and Evolution of Disk Galaxies: Cosmological Initial Conditions and the Gravitational Collapse. *ApJ*, 505:37–49, September 1998.

4. R. C. Kraan-Korteweg et al. 21 CM line widths and distances of spiral galaxies. In B. F. Madore and R. B. Tully, editors, *NATO ASIC Proc. 180: Galaxy Distances and Deviations from Universal Expansion*, pp. 65–72, 1986.
5. K. O’Neil et al. Red, Gas-Rich Low Surface Brightness Galaxies and Enigmatic Deviations from the Tully-Fisher Relation. *AJ*, 119:136–152, January 2000.
6. S. S. McGaugh et al. The Baryonic Tully-Fisher Relation. *ApJL*, 533:L99–L102, April 2000.
7. S. S. McGaugh. The Baryonic Tully-Fisher Relation of Galaxies with Extended Rotation Curves and the Stellar Mass of Rotating Galaxies. *ApJ*, 632:859–871, October 2005.
8. S. Courteau et al. Scaling Relations of Spiral Galaxies. *ApJ*, 671:203–225, December 2007.
9. K. Said et al. On how to extend the NIR Tully-Fisher relation to be truly all-sky. *MNRAS*, 447(2):1618–1629, February 2015.
10. C. M. Springob et al. SFI++. II. A New I-Band Tully-Fisher Catalog, Derivation of Peculiar Velocities, and Data Set Properties. *ApJS*, 172:599–614, October 2007.
11. K. L. Masters et al. 2MTF. I. The Tully-Fisher Relation in the Two Micron all Sky Survey J, H, and K Bands. *AJ*, 135:1738–1748, May 2008.
12. R. B. Tully et al. The Extragalactic Distance Database. *AJ*, 138(2):323–331, August 2009.
13. H. M. Courtois et al. Cosmography of the Local Universe. *AJ*, 146:69, September 2013.
14. T. Hong et al. 2MTF - VII. 2MASS Tully-Fisher survey final data release: distances for 2062 nearby spiral galaxies. *MNRAS*, 487(2):2061–2069, August 2019.
15. H. M. Courtois et al. WALLABY pre-pilot and pilot survey: The Tully Fisher relation in Eridanus, Hydra, Norma, and NGC4636 fields. *MNRAS*, 519(3):4589–4607, March 2023.
16. P. Boubel et al. Cosmic growth rate measurements from Tully-Fisher peculiar velocities. *arXiv e-prints*, pp. arXiv:2301.12648, January 2023.
17. E. Opik. An estimate of the distance of the Andromeda Nebula. *ApJ*, 55:406–410, June 1922.
18. C. Balkowski et al. Neutral hydrogen study of spiral and irregular dwarf galaxies. *A&A*, 34:43–52, August 1974.
19. S. Djorgovski and M. Davis. Fundamental properties of elliptical galaxies. *ApJ*, 313:59–68, February 1987.
20. A. Dressler et al. Spectroscopy and photometry of elliptical galaxies - A large-scale streaming motion in the local universe. *ApJL*, 313:L37–L42, February 1987.
21. A. Sandage and G. A. Tammann. Steps toward the Hubble constant. V. The Hubble constant from nearby galaxies and the regularity of the local velocity field. *ApJ*, 196:313–328, March 1975.
22. G. de Vaucouleurs and G. Bollinger. The extragalactic distance scale. VII. The velocity-distance relations in different directions and the Hubble ratio within and without the local supercluster. *ApJ*, 233:433–452, October 1979.
23. S. Zaroubi et al. Wiener Reconstruction of the Large-Scale Structure. *ApJ*, 449:446, August 1995.
24. R. B. Tully et al. The Laniakea supercluster of galaxies. *Nature*, 513(7516):71–73, September 2014.
25. R. B. Tully et al. Cosmicflows-4. *ApJ*, 944(1):94, February 2023.
26. H. M. Courtois et al. Gravity in the local Universe: Density and velocity fields using CosmicFlows-4. *A&A*, 670:L15, February 2023.
27. A. Dupuy and H. M. Courtois. Watersheds of the Universe: Laniakea and five newcomers in the neighborhood. *arXiv e-prints*, pp. arXiv:2305.02339, May 2023.
28. P. Andersen et al. Cosmology with peculiar velocities: observational effects. *MNRAS*, 463(4):4083–4092, December 2016.
29. R. Watkins et al. Consistently large cosmic flows on scales of  $100h^{-1}$  Mpc: a challenge for the standard  $\Lambda$ CDM cosmology. *MNRAS*, 392(2):743–756, January 2009.
30. R. Watkins et al. Analyzing the Large-Scale Bulk Flow using CosmicFlows4: Increasing Tension with the Standard Cosmological Model. *arXiv e-prints*, pp. arXiv:2302.02028, February 2023.
31. A. M. Whitford et al. Evaluating bulk flow estimators for CosmicFlows-4 measurements. *arXiv e-prints*, pp. arXiv:2306.11269, June 2023.

32. M. Davis et al. Local gravity versus local velocity: solutions for  $\beta$  and non-linear bias. *MNRAS* , 413(4):2906–2922, June 2011.
33. J. Carrick et al. Cosmological parameters from the comparison of peculiar velocities with predictions from the 2M++ density field. *MNRAS* , 450(1):317–332, June 2015.
34. J. F. Navarro and M. Steinmetz. Dark Halo and Disk Galaxy Scaling Laws in Hierarchical Universes. *ApJ* , 538(2):477–488, August 2000.
35. M. Vogelsberger et al. Properties of galaxies reproduced by a hydrodynamic simulation. *Nature* , 509(7499):177–182, May 2014.
36. A. A. Ponomareva et al. From light to baryonic mass: the effect of the stellar mass-to-light ratio on the Baryonic Tully-Fisher relation. *MNRAS* , 474(4):4366–4384, March 2018.
37. J. F. Navarro et al. The Structure of Cold Dark Matter Halos. *ApJ* , 462:563, May 1996.
38. H. J. Mo and S. Mao. The Tully-Fisher relation and its implications for the halo density profile and self-interacting dark matter. *MNRAS* , 318(1):163–172, October 2000.
39. U. Seljak. Constraints on galaxy halo profiles from galaxy-galaxy lensing and Tully-Fisher/Fundamental Plane relations. *MNRAS* , 334(4):797–804, August 2002.
40. M. Aaronson et al. The infrared luminosity/H I velocity-width relation and its application to the distance scale. *ApJ* , 229:1–13, April 1979.
41. N. Bouché and S. E. Schneider. IR-TF Relation in the Zone of Avoidance with 2MASS. In R. C. Kraan-Korteweg et al., editors, *Mapping the Hidden Universe: The Universe behind the Milky Way - The Universe in HI*, volume 218 of *Astronomical Society of the Pacific Conference Series*, pp. 111, January 2000.
42. K. Said et al. NIR Tully-Fisher in the Zone of Avoidance - III. Deep NIR catalogue of the HIZOA galaxies. *MNRAS* , 462(3):3386–3400, November 2016.
43. M. J. Pierce and R. B. Tully. Distances to the Virgo and Ursa Major Clusters and a Determination of  $H_0$ . *ApJ* , 330:579, July 1988.
44. H. M. Courtois et al. The Extragalactic Distance Database: All Digital H I Profile Catalog. *AJ* , 138(6):1938–1956, December 2009.
45. R. Giovanelli et al. The I Band Tully-Fisher Relation for Cluster Galaxies: a Template Relation, its Scatter and Bias Corrections. *AJ* , 113:53–79, January 1997.
46. K. L. Masters et al. SFI++ I: A New I-Band Tully-Fisher Template, the Cluster Peculiar Velocity Dispersion, and  $H_0$ . *ApJ* , 653(2):861–880, December 2006.
47. K. Said et al. NIR Tully-Fisher in the Zone of Avoidance - II. 21 cm H I-line spectra of southern ZOA galaxies. *MNRAS* , 457(3):2366–2376, April 2016.
48. R. Bell et al. Calibration of the Tully-Fisher relation in the WISE W1 (3.4  $\mu\text{m}$ ) and W2 (4.6  $\mu\text{m}$ ) bands. *MNRAS* , 519(1):102–120, February 2023.
49. M. A. W. Verheijen. The Ursa Major Cluster of Galaxies. V. H I Rotation Curve Shapes and the Tully-Fisher Relations. *ApJ* , 563(2):694–715, December 2001.
50. F. Lelli et al. The baryonic Tully-Fisher relation for different velocity definitions and implications for galaxy angular momentum. *MNRAS* , 484(3):3267–3278, April 2019.
51. J. A. Willick et al. Homogeneous Velocity-Distance Data for Peculiar Velocity Analysis. I. Calibration of Cluster Samples. *ApJ* , 446:12, June 1995.
52. J. A. Willick et al. Homogeneous Velocity-Distance Data for Peculiar Velocity Analysis. II. Calibration of Field Samples. *ApJ* , 457:460, February 1996.
53. D. W. Hogg et al. Data analysis recipes: Fitting a model to data. *arXiv e-prints*, pp. arXiv:1008.4686, August 2010.
54. M. A. Strauss and J. A. Willick. The density and peculiar velocity fields of nearby galaxies. *Phys. Rep.*, 261:271–431, January 1995.
55. J. Mould. Understanding the Fundamental Plane and the Tully Fisher Relation. *Frontiers in Astronomy and Space Sciences*, 7:21, May 2020.
56. M. Milgrom. A modification of the Newtonian dynamics as a possible alternative to the hidden mass hypothesis. *ApJ* , 270:365–370, July 1983.
57. F. C. van den Bosch and J. J. Dalcanton. Semianalytical Models for the Formation of Disk Galaxies. II. Dark Matter versus Modified Newtonian Dynamics. *ApJ* , 534(1):146–164, May 2000.

58. F. C. van den Bosch and J. J. Dalcanton. Disk Galaxies as Cosmological Benchmarks: Cold Dark Matter versus Modified Newtonian Dynamics. In J. G. Funes and E. M. Corsini, editors, *Galaxy Disks and Disk Galaxies*, volume 230 of *Astronomical Society of the Pacific Conference Series*, pp. 549–552, January 2001.
59. J. Schaye et al. The EAGLE project: simulating the evolution and assembly of galaxies and their environments. *MNRAS*, 446(1):521–554, January 2015.
60. E. Papastergis et al. An accurate measurement of the baryonic Tully-Fisher relation with heavily gas-dominated ALFALFA galaxies. *A&A*, 593:A39, September 2016.
61. S. Courteau and H.-W. Rix. Maximal Disks and the Tully-Fisher Relation. *ApJ*, 513(2):561–571, March 1999.
62. N. N. Q. Ouellette et al. The Spectroscopy and H-band Imaging of Virgo Cluster Galaxies (SHIVir) Survey: Scaling Relations and the Stellar-to-total Mass Relation. *ApJ*, 843(1):74, July 2017.
63. B. Abolfathi et al. The Fourteenth Data Release of the Sloan Digital Sky Survey: First Spectroscopic Data from the Extended Baryon Oscillation Spectroscopic Survey and from the Second Phase of the Apache Point Observatory Galactic Evolution Experiment. *ApJS*, 235(2):42, April 2018.
64. C. Lintott et al. Galaxy Zoo 1: data release of morphological classifications for nearly 900 000 galaxies. *MNRAS*, 410(1):166–178, January 2011.
65. A. Carr et al. The Pantheon+ analysis: Improving the redshifts and peculiar velocities of Type Ia supernovae used in cosmological analyses. *PASA*, 39:e046, October 2022.
66. D. Brout et al. The Pantheon+ Analysis: Cosmological Constraints. *ApJ*, 938(2):110, October 2022.
67. A. G. Riess et al. A 2.4% Determination of the Local Value of the Hubble Constant. *ApJ*, 826(1):56, July 2016.
68. S. S. McGaugh. The Baryonic Tully-Fisher Relation of Gas-rich Galaxies as a Test of  $\Lambda$ CDM and MOND. *AJ*, 143(2):40, February 2012.
69. F. Lelli et al. The Small Scatter of the Baryonic Tully-Fisher Relation. *ApJL*, 816(1):L14, January 2016.
70. D. Obreschkow and M. Meyer. Precise Tully-Fisher Relations without Galaxy Inclinations. *ApJ*, 777(2):140, November 2013.
71. N. Visvanathan. A global value of the Hubble constant. *ApJ*, 275:430–444, December 1983.
72. A. Sandage and G. A. Tammann. The Hubble constant as derived from 21 cm linewidths. *Nature*, 307(5949):326–329, January 1984.
73. A. Sandage and G. A. Tammann. Steps toward the Hubble constant. VIII - The global value. *ApJ*, 256:339–345, May 1982.
74. M. Aaronson et al. A Distance Scale from the Infrared Magnitude/ H i Velocity-Width Relation. V. Distance Moduli to 10 Galaxy Clusters, and Positive Detection of Bulk Supercluster Motion toward the Microwave Anisotropy. *ApJ*, 302:536, March 1986.
75. R. C. Kraan-Korteweg et al. 21 Centimeter Line Width Distances of Cluster Galaxies and the Value of H 0. *ApJ*, 331:620, August 1988.
76. M. Fukugita et al. The Distance to the Coma Cluster Using the B-Band Tully-Fisher Relation. *ApJ*, 376:8, July 1991.
77. H. J. Rood and B. A. Williams. Tully-Fisher distances to M31-like galaxies in the Coma cluster. *MNRAS*, 263:211–228, July 1993.
78. M. Bureau et al. A New I-Band Tully-Fisher Relation for the Fornax Cluster: Implication for the Fornax Distance and Local Supercluster Velocity Field. *ApJ*, 463:60, May 1996.
79. B. F. Madore et al. The Hubble Space Telescope Key Project on the Extragalactic Distance Scale. XV. A Cepheid Distance to the Fornax Cluster and Its Implications. *ApJ*, 515(1):29–41, April 1999.
80. S. Sakai et al. The Hubble Space Telescope Key Project on the Extragalactic Distance Scale. XXIV. The Calibration of Tully-Fisher Relations and the Value of the Hubble Constant. *ApJ*, 529(2):698–722, February 2000.
81. W. L. Freedman et al. Final Results from the Hubble Space Telescope Key Project to Measure the Hubble Constant. *ApJ*, 553(1):47–72, May 2001.

82. R. B. Tully and H. M. Courtois. Cosmicflows-2: I-band Luminosity-H I Linewidth Calibration. *ApJ* , 749(1):78, April 2012.
83. J. G. Sorce et al. The Mid-infrared Tully-Fisher Relation: Calibration of the Type Ia Supernova Scale and  $H_0$ . *ApJL* , 758(1):L12, October 2012.
84. J. G. Sorce et al. Calibration of the Mid-infrared Tully-Fisher Relation. *ApJ* , 765(2):94, March 2013.
85. J. D. Neill et al. The Calibration of the WISE W1 and W2 Tully-Fisher Relation. *ApJ* , 792(2):129, September 2014.
86. J. G. Sorce et al. From Spitzer Galaxy photometry to Tully-Fisher distances. *MNRAS* , 444(1):527–541, October 2014.
87. E. Kourkchi et al. Cosmicflows-4: The Calibration of Optical and Infrared Tully-Fisher Relations. *ApJ* , 896(1):3, June 2020.
88. E. Kourkchi et al. Cosmicflows-4: the baryonic Tully-Fisher relation providing 10 000 distances. *MNRAS* , 511(4):6160–6178, April 2022.
89. A. G. Riess et al. A Comprehensive Measurement of the Local Value of the Hubble Constant with  $1 \text{ km s}^{-1} \text{ Mpc}^{-1}$  Uncertainty from the Hubble Space Telescope and the SH0ES Team. *ApJL* , 934(1):L7, July 2022.
90. Planck Collaboration et al. Planck 2018 results. VI. Cosmological parameters. *A&A*, 641:A6, September 2020.
91. M. Watanabe et al. Surface Photometric Calibration of the Infrared Tully-Fisher Relation Using Cepheid-based Distances of Galaxies. *ApJ* , 555(1):215–231, July 2001.
92. D. G. Russell. The Ks-band Tully-Fisher relation - A determination of the Hubble parameter from 218 ScI galaxies and 16 galaxy clusters. *Journal of Astrophysics and Astronomy*, 30:93–118, August 2009.
93. L. Bottinelli et al. Cluster population incompleteness bias and the value of  $H_0$  from the Tully-Fisher B relation. *A&A*, 181:1–13, July 1987.
94. L. Hislop et al. The Extragalactic Distance Scale without Cepheids. IV. *ApJ* , 733(2):75, June 2011.
95. L. Bottinelli et al. The value of  $H_0$  from the infrared Tully-Fisher relation. *A&A*, 196:17–25, May 1988.
96. J. Schombert et al. Using the Baryonic Tully-Fisher Relation to Measure  $H_0$ . *AJ* , 160(2):71, August 2020.
97. R. B. Tully and M. J. Pierce. Distances to Galaxies from the Correlation between Luminosities and Line Widths. III. Cluster Template and Global Measurement of  $H_0$ . *ApJ* , 533(2):744–780, April 2000.
98. C. Saulder et al. Target Selection for the DESI Peculiar Velocity Survey. *arXiv e-prints*, pp. arXiv:2302.13760, February 2023.